J Physiol Sci (2009) 59:317–328
DOI 10.1007/s12576-009-0039-5

ORIGINAL PAPER

Factors affecting SOCE activation in mammalian skeletal muscle fibers

Pura Bolaños · Alis Guillén · Reinaldo DiPolo · Carlo Caputo

Received: 19 January 2009 / Accepted: 13 April 2009 / Published online: 14 May 2009

Abstract Enzymatically dissociated mouse FDB muscle fibers, loaded with Fura-2 AM, were used to study the effect of mitochondrial uncoupling on the capacitative Ca^{2+} entry, SOCE. Sarcoplasmic reticulum (SR) Ca^{2+} stores were depleted by repetitive exposures to high K^+ or 4-chloro-m-Cresol (4-CmC) in the absence of extracellular Ca^{2+}. SR Ca^{2+} store replenishment was substantially reduced using 5 μM cyclopiazonic acid (CPA). Readmission of external Ca^{2+} (5 mM) increased basal $[Ca^{2+}]_i$ under two modalities. In mode 1 $[Ca^{2+}]_i$ initially increased at a rate of 0.8 ± 0.1 nM/s and later at a rate of 12.3 ± 2.6 nM/s, reaching a final value of 477.8 ± 36.8 nM in 215.7 ± 25.9 s. In mode 2, $[Ca^{2+}]_i$ increased at a rate of 0.8 ± 0.1 nM/s to a value of 204.9 ± 20.6 nM in 185.4 ± 21.1 s. FCCP, 2 μM, reduced this Ca^{2+} entry. In nine FCCP-poisoned fibers, the initial rate of Ca^{2+} increase was 0.34 ± 0.1 nM/s (mean ± SEM), reaching a plateau of 149.2 ± 14.1 nM in 217 ± 19 s. The results may likely be explained by the hypothesis that SOCE is inhibited by mitochondrial uncouplers, pointing to a possible mitochondrial role in its activation. Using time-scan confocal microscopy and the dyes CaOr-5N AM or Rhod-2 AM to label mitochondrial Ca^{2+}, we show that during depletion $[Ca^{2+}]_{mito}$ initially increases and later diminishes. Finally, we show that the increase in basal $[Ca^{2+}]_i$, associated with SOCE activation, diminishes upon external Na^+ withdrawal. Na^+ entry through the SOCE pathway and activation of the reversal of Na^+/Ca^{2+} exchanger could explain this SOCE modulation by Na^+.

P. Bolaños (✉) · A. Guillén · R. DiPolo · C. Caputo
Laboratorio de Fisiología Celular, Centro de Biofísica y Bioquímica, Instituto Venezolano de Investigaciones Científicas IVIC, Apartado 20632, Caracas 1020A, Venezuela
e-mail: pbolanos@ivic.ve

Keywords Skeletal muscle · Mitochondria · SOCE · Ca^{2+} imaging · Na^+/Ca^{2+} exchange

Introduction

In many cells Ca^{2+} entry occurs through a pathway whose activation is dependent on the Ca^{2+} content of intracellular stores. This Ca^{2+} influx, known as capacitative Ca^{2+} entry or store operated Ca^{2+} entry (SOCE), was first described and well characterized in non-excitable cells, where it constitutes a major pathway for Ca^{2+} influx [1, 2]. The electrical manifestation of this Ca^{2+} entry in the continuous presence of extracellular Ca^{2+} is represented by a Ca^{2+} current, Icrac, that flows through channels activated by substantial depletion of endoplasmic reticulum (ER) Ca^{2+} stores, normally operated by IP3 receptors [2–6].

This mode of Ca^{2+} entry has also been described in excitable cells, as is the case for adult skeletal muscle fibers, where the sarcoplasmic reticulum (SR) calcium stores are operated by ryanodine receptors. The presence of SOCE in adult skeletal muscle fibers has been reported by different authors using different techniques [7–12]. However, attempts to measure SOCE single channel currents during SR Ca^{2+} release and/or SR Ca^{2+} depletion of muscle fibers under cell attached patch conditions have produced conflicting results [10, 13]. The reason for this could lie in the small magnitude of the currents with Ca^{2+} as the charge carrier and their preferential localization at level of the t-tubules membrane [11]. The physiological role of SOCE in skeletal muscle is not well understood, although it has been suggested that it could be relevant for replenishing exhausted SR Ca^{2+} stores during prolonged contractile activity. Furthermore, there is much less information on the regulatory mechanisms involved in SOCE

activation in excitable cells, in particular adult skeletal muscle fibers, than in non-excitable cells. The main aim of this work was to study the effect of mitochondrial poisoning with FCCP on SOCE in mouse skeletal muscle fibers. We have measured SOCE in terms of cytoplasmic Ca^{2+} increases in the presence of CPA, a potent inhibitor of the Ca^{2+} SR pump. We show, for the first time that, in adult mouse skeletal muscle fibers, mitochondria poisoning by FCCP reduces the cytoplasmic Ca^{2+} increase likely to be associated with SOCE. Furthermore, we present some evidence that mitochondria may take up Ca^{2+} during the early stages of the store depletion procedure, but release it when depletion is completed, thus suggesting the possibility of cross-talking between SR and mitochondria. Finally, we have tested the possibility that also in mice muscle fibers, as occurs in human platelets [14], Na^+ entry might occur simultaneously with SOCE, promoting additional Ca^{2+} entry through the operation of the Na^+/Ca^{2+} exchanger in its reverse mode.

Methods

Fiber preparation

The enzymatic dissociation method was similar to the one previously published [15, 16]. Briefly, *flexor digitorum brevis* (FDB) muscles were dissected from adult (42 days) mice (NMR IVIC). The mice were killed by rapid cervical dislocation. Procedures were approved by the local animal care committee. Muscles were incubated in a modified mammalian Ringer solution (see below) containing 1 mM Ca^{2+} and 4 mg/ml collagenase (*Worthington CLS2*) for 1 h at 36°C. After incubation with collagenase, the muscles were washed three times with the 1 mM Ca^{2+} Ringer's solution and gently separated from tendons and remaining tissue with a fire-polished Pasteur pipette. All the experiments were carried out at room temperature (20–22°C).

Experimental solutions and chemicals

The composition of the basic experimental solution (mammalian normal Ringer's solution, NR) was as follows (in mM): 145 NaCl, 2.5 KCl, 1.0 $MgSO_4$, 2.5 $CaCl_2$, 10 D-glucose, 10 HEPES, pH 7.4. The 5 Ca^{2+} solution was the same as NR but with 5 mM $CaCl_2$. Ca^{2+}-free (0Ca) solution had the following composition (in mM): 145 NaCl, 2.8 KCl, 2 $MgSO_4$, 10 D-glucose, 10 HEPES, 0.5 EGTA, pH 7.4, 290 mOsm. The high K^+–0Ca^{2+} solution had the following composition (in mM): 75 K_2SO_4, 5 NaCl, 2 $MgSO_4$, 10 HEPES, 10 glucose, pH 7.4.

Carbonyl cyanide 4-(trifluoromethoxy) phenylhydrazone (FCCP), cyclopiazonic acid (CPA), *N*-benzyl-*p*toluene sulphonamide (BTS) (Sigma St Louis, MO), 4-chloro-m-Cresol (4-CmC) (Fluka Chemical Corp, RonKonKoma, NY), 2-aminoethoxydiphenyl borate (2-APB)(Calbiochem, La Jolla, CA) and KB-R7943 (EMD Biosciences, Inc. San Diego, CA) were added from stock solutions to the concentrations indicated. All fluorescent dyes, Fura-2 AM, Rhod-2 AM, Calcium Orange-5N AM, MitoTracker® Green FM and SBFI AM (benzofuran isophthalate), were from Molecular Probes (Eugene, OR). They were dissolved in DMSO at a final concentration of 0.1%.

Depletion protocol

The fiber viability was verified by electrical stimulation followed by exposures to high K^+ solution prior to depleting the SR Ca^{2+} stores of fibers poisoned with cyclopiazonic acid. This procedure consisted of a series of exposures either individually or in combination with high K^+ for 1–3 s, or with the ryanodine receptor agonist 4-CmC (500 μM) for 10–40 s, in the absence of external Ca^{2+}. The criterion for depletion was based on the drastic reduction of the Ca^{2+} transient responses to the high K^+ or the 4-CmC challenges as illustrated in Fig. 1. In 29 different fibers, the number of exposures to the high K^+ and/or 4-CmC was 9.8 ± 0.5, (mean ± SEM, $n = 29$).

Movement artifacts

As previously shown [16], Ca^{2+} transients can be recorded with few movement artifacts by selecting fibers that spontaneously adhered to the glass cover slide bottom of the experimental chamber. To further reduce movement artifacts, all experimental solutions contained 40 μM BTS to diminish contraction. This was particularly important in confocal microscopy experiments, since we intended to carry out measurements of changes in mitochondrial Ca^{2+}-dependent fluorescence in the same fiber region during the depletion procedure. In this case, we also coated the glass cover slides with 1 mg/ml laminin (Sigma) to improve attachment of the fibers and allowed them to rest between 2 and 3 h before starting the experiment.

Fluorescence recording

Fura-2 basal Ca^{2+} measurements

Dissociated fibers were loaded with the Ca^{2+}-sensitive fluorescent indicator Fura-2 AM 5 μM (Molecular Probes) for 30 min at room temperature in the dark and then washed with standard solution. Once placed in the experimental chamber, the loaded cells were allowed to rest an additional 15 min to allow further de-esterification.

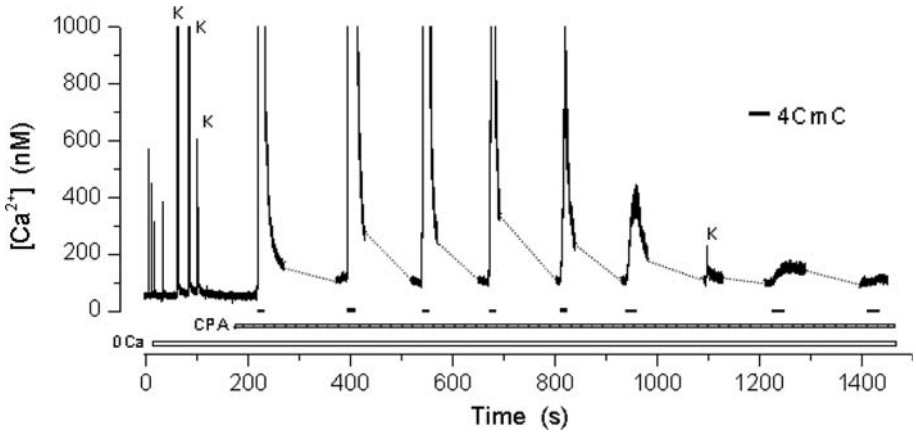

Fig. 1 Depletion procedure. One fiber, bathed in a 0 Ca^{2+} medium, was electrically stimulated four times and challenged three times with the high K^+ solution to verify its viability before treating it with CPA. In the presence of this agent, the fiber was exposed several times to 4-CmC until the responses to high K^+ and to 4-CmC were practically abolished. In this and following figures, the dashed lines represent acquisition interruptions. A similar protocol, not entirely shown, preceded the traces of the experiments of Figs. 2, 3, 4, 5 and 8

Fura-2 fluorescence was measured with a fluorescence imaging apparatus (Ionoptix Co., Milton, MA) mounted on an inverted Nikon Diaphot TMD microscope. For fura-2 measurements the light from a 100-W xenon lamp was filtered alternating 340/20- and 380/18-nm interference filters (Chroma Technology Corp., Rockingham, VT). The resultant fluorescence was passed through a 400-nm dichroic mirror, filtered at 510/40 nm (Chroma Technology Corp., Rockingham, VT) and collected using an intensified CCD camera. Fluorescence images were taken at a rate of 33 ms/frame, digitalized and analyzed using the IonOptix software. The Ca^{2+} concentration was calculated according to the formula [17]:

$$[Ca^{2+}]_i = K_d \cdot (R - R_{min})/(R_{max} - R) \cdot Sf_2/Sb_2$$

where R is the measured fluorescence ratio. The values of R_{max} and R_{min} and the constant Sf_2/Sb_2 (fluorescence of free and Ca^{2+}-bound fura-2 at 380 nm) were calculated in vitro using variable CaEGTA/EGTA ratios to give different $[Ca^{2+}]$ (Kit no. 1, Molecular Probes). The dissociation constant K_d, for the fura-Ca^{2+} complex, was taken as 89 nM, which is a value obtained from the on and off rate constants for calcium binding to fura-2 in muscle fibers [18].

Since with our configuration, the equipment allowed the acquisition of images at video rate, the Ca^{2+} transients elicited by electrical stimulation were heavily filtered and are only shown as proof of fiber excitability.

SBFI sodium measurements

The dissociated muscle fibers were loaded with the membrane-permeable acetoxy methyl ester of the fluorescent sodium-binding benzofuran isophthalate, SBFI-AM (Molecular Probes). Stock solution was prepared by dissolving SBFI-AM in dimethyl sulphoxide (DMSO) to a concentration of 2 mM. The loading solution was made by adding 2 µl of 25% wt/wt Pluronic F-127 (Molecular Probes) in DMSO to 3 µl of SBFI-AM stock solution, sonicated and then diluted in 1 ml of NR. The final concentration of SBFI-AM in the solution was 6 µM [19]. The dye was excited at 340/20 and 383/18 nm wavelengths, and emitted light was recorded at 510/40 nm. Only fibers that responded to electrical stimulation were selected.

Laser scanning confocal microscopy

Cells loaded with Calcium Orange-5N AM (CaOr-5N) or with Rhod-2 AM fluorescent dyes were plated on cover slides coated with laminine as described above. The cover slide was placed as the bottom of the superfusion open chamber mounted on the stage of an inverted Nikon Eclipse TE2000 microscope equipped with a Plan Fluor 100× 1.3 NA oil-immersion objective and coupled to a laser scanning confocal system Nikon C1, with Neon (543 nm) and air-cooled Argon (488) lasers, 515/530 (BP) and 570 (LP) emission filters.

Mitochondria were observed in cells loaded with 200 nM MitoTracker Green FM, a cell permeant mitochondrion selective dye (490 nm excitation/516 nm emission) that passively diffuses across the plasma membrane and accumulates in the lipid environment of mitochondria (Molecular Probes) [20].

Time-scan confocal microscopy was used in individual cells to follow mitochondrial calcium ($[Ca^{2+}]_{mito}$) changes during the depletion procedure. To follow $[Ca^{2+}]_{mito}$ changes, dissociated fibers were loaded with 5 µM CaOr-5N AM, K_d 87 µM [21] for 60 min at 37°C or 7 µM Rhod-2 AM, K_d 570 nM (Molecular Probes) for 120 min at 37°C in mammalian Ringer's solution, washed and then

incubated for an additional 10 min at 37°C. Data were acquired with the Nikon EZ-C1 software and processed with the Nikon Viewer 1.00. Mitochondrial fluorescence intensity was obtained using the particle analysis facility of the ImageJ 1.41 g program (Free Software, National Institutes of Health). This program allows recognition and measurement of the area of the selected objects for analysis, giving the brightness value for each pixel. As shown in Fig. 7b, basically all the mitochondria present in the confocal image could be selected for analysis.

Results

Ca^{2+}-dependent $[Ca^{2+}]_{myo}$ increase in SR Ca^{2+} depleted fibers

Figure 1 shows that following depletion, the basal myoplasmic Ca^{2+} concentration $[Ca^{2+}]_{myo}$ was somewhat higher than before depletion. In all figures, the dashed lines represent breaks in acquisition in order to diminish illumination periods and prevent fiber photo-damage. Table 1 shows that after depleting the SR Ca^{2+} stores, $[Ca^{2+}]_{myo}$ increased from an initial value of 61 ± 2 to 86 ± 3 nM (mean ± SEM, $n = 29$).

Following depletion of the SR Ca^{2+} stores in the absence of external Ca^{2+}, exposure of the fibers to a solution containing 5 mM Ca^{2+} caused an increase in the $[Ca^{2+}]_{myo}$. This increase occurred mainly under two different modalities as illustrated in Fig. 2. In this and the following figures, the experimental record started once depletion was completed. Figure 2a shows the result of a run in which, following exposure to 5 mM Ca^{2+}, the $[Ca^{2+}]_{myo}$ started to rise at first slowly and then increasingly faster from an initial level of about 80 nM to a value of about 500 nM in 280 s. At this point the fiber was exposed to the normal Ringer's solution (NR) containing 2 mM Ca^{2+} and no CPA, which caused a relatively fast decay of the $[Ca^{2+}]_{myo}$ to a quasi-basal condition. The interruption of the $[Ca^{2+}]_{myo}$ increase in response to 5 mM Ca^{2+} was necessary to avoid reaching higher $[Ca^{2+}]_{myo}$ that would have resulted in fiber contraction and the end of the experiment. We define this type of response as mode 1. Figure 2b shows the result of another experiment in which following exposure to the 5 mM external Ca^{2+} solution, the $[Ca^{2+}]_{myo}$ increased slowly from an initial level of about 75 nM to a plateau level of about 170 nM in 156 s, which was reversed upon exposure of the fiber to NR. This is defined as a mode 2 response. In both cases, the fibers fully reacquired their capacity to respond to high K^+ solution after a recovery period of about 180 s. Table 1 shows that in 29 fibers tested, 14 showed a mode 1 response, while 15 responded in mode 2. The table also shows that for the fibers responding in mode 1, the initial and final rates of $[Ca^{2+}]_{myo}$ increase were respectively 0.8 ± 0.1 and 12.3 ± 3 nM/s, while the $[Ca^{2+}]_{myo}$ attained before the response interruption was 477.8 ± 36.8 nM. The time to reach this value was 215.7 ± 25.9 s. In the case of fibers responding in mode 2, the initial rate of $[Ca^{2+}]_{myo}$ increase was 0.8 nM/s, while the plateau $[Ca^{2+}]_{myo}$ value was 204.9 ± 20.6 nM, attaining this value in 185.4 ± 21.1 s.

Figure 3 shows three runs carried out with different fibers in which CPA was washed out at varying times during the experiment. Figure 3a shows that after completing the depletion procedure, the fiber was exposed to 5 mM Ca^{2+}, which caused the basal $[Ca^{2+}]_{myo}$ to increase from 110 to 231 nM. CPA was washed out 176 s after exposure to 5 mM Ca^{2+} and, after a delay of about 10 s, $[Ca^{2+}]_{myo}$ began to decrease, reaching the baseline level in about 110 s. In Fig. 3b, CPA was withdrawn simultaneously with the exposure to 5 mM Ca^{2+}, resulting in a small and transient increase of $[Ca^{2+}]_{myo}$ from 103 to 138 nM followed by a spontaneous decay to the initial value. This decay could be due to Ca^{2+} uptake by the SR, and soon after washing out CPA competes with SOCE. This would explain the recovery of the K^+ contracture elicited after switching to the 0 Ca^{2+} condition. In Fig. 3c, CPA was washed out 74 s before exposure to the 5 mM Ca^{2+} solution; in this case the $[Ca^{2+}]_{myo}$ increase was almost abolished. In addition to showing the reversibility of the CPA effect, these results demonstrate that in the absence of CPA, the SR Ca^{2+} pump is an effective buffer that successfully competes with the mechanism responsible for the described Ca^{2+} increase.

Table 1 Effect of FCCP on SOCE

	$[Ca^{2+}]_{bsl}$		$[Ca^{2+}]_{myo}$ increase			
	Pre-deplet (nM)	Post-deplet (nM)	Initial rate (nM/s)	Final rate (nM/s)	Final level (nM)	
			Modes 1 and 2	Mode 1	Mode 1	Mode 2
Control	61.1* ± 2.4 (29)*	85.9 ± 2.7 (29)	0.8 ± 0.1 (29)	12.3 ± 2.6 (14)	477.8 ± 36.8 (14)	204.9 ± 20.6 (15)
FCCP	67.1 ± 5.1 (11)	85.5 ± 4.1 (11)	0.3 ± 0.1 (11)	–	–	149.2 ± 14.0 (11)

* Mean ± SEM (*N*)

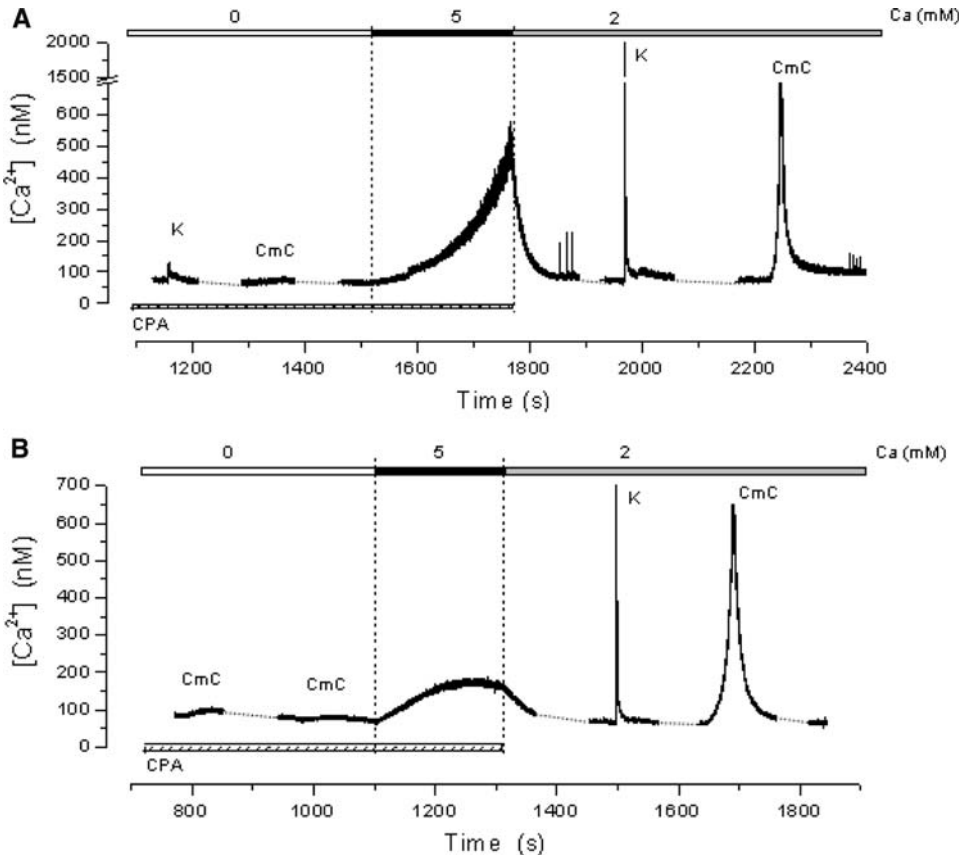

Fig. 2 Two modalities of SOCE activation. Following depletion of the SR Ca^{2+} stores, achieved in the absence of external Ca^{2+}, exposing the fibers to a solution containing 5 mM Ca^{2+}, causes an increase in the $[Ca^{2+}]_{myo}$ that basically follows two different modalities. Trace in **a** shows an experiment in which $[Ca^{2+}]_{myo}$, after a slow start, increases rapidly to a value higher than 500 nM, rendering it necessary to reverse it to avoid fiber contracture and damage, mode 1. Trace in **b** shows that in another fiber, the $[Ca^{2+}]_{myo}$ increase is slower and saturates at a lower value, mode 2. The characteristics parameters of the two modes are resumed in Table 1. Notice the recovery of the responses to K^+ and 4-CmC at the end of the runs

Mechanism of $[Ca^{2+}]_{myo}$ increase

In order to identify the mechanism responsible for the $[Ca^{2+}]_{myo}$ increase following depletion of intracellular Ca^{2+} stores, we used 2-APB at high concentration and Gd^{3+}, known inhibitors of SOCE.

Figure 4 shows the effect of 2-APB in two different fibers. Trace A shows that exposure to 80 μM 2-APB, partially reversed the $[Ca^{2+}]_{myo}$ increase induced by 2 mM Ca^{2+} in a depleted fiber. Trace B shows that after completing the depletion procedure, simultaneous exposure of the fiber to 5 mM Ca^{2+} and 2-APB failed to cause the $[Ca^{2+}]_{myo}$ increase. A small delayed increase could be observed after washing out the drug.

Similar results were obtained with 10 μM Gd^{3+} that effectively reverted the $[Ca^{2+}]_{myo}$ increase induced by 5 mM Ca^{2+} in a depleted fiber. In other experiments, addition of Gd^{3+} completely prevented the $[Ca^{2+}]_{myo}$ increase when it was applied before the addition of 5 mM Ca^{2+}. We also used Mn^{2+}, which was effective in reducing fura-2 fluorescence, as indicated by the reversal of the 340/380 ratio increase after stimulation with 5 mM Ca^{2+} (experiments not shown). Mn^{2+} is used to reveal ICRAC in non-excitable cells where there are no other Ca^{2+} entry pathways [22]. The observed $[Ca^{2+}]_{myo}$ increase was not affected by 10 μM nifedipine or 10 μM D-600, well known blockers of the L-type Ca^{2+} channels. The above experiments suggest that the $[Ca^{2+}]_{myo}$ increase observed in depleted fibers exposed to 2.5 or 5 mM Ca^{2+} is mediated by Ca^{2+} entry through SOCE.

Effects of FCCP on $[Ca^{2+}]_{myo}$ increase mediated by SOCE

Figure 5a shows an experiment in which treatment of a fiber with 2 μM FCCP for 2 min, after Ca^{2+} store depletion under $0Ca^{2+}$ conditions, caused a small increase in $[Ca^{2+}]_{myo}$. Exposure to 5 mM external Ca^{2+} caused a further increase, which was however considerably smaller than those obtained in the absence of FCCP (see Fig. 2b). The last portion of the record shows that after a recovery period, the fiber responded to high K^+. Table 1 summarizes the results obtained in several experiments of this type. The results indicate that mitochondrial poisoning effectively diminishes SOCE activation. Experiments were carried out to test whether FCCP could affect SOCE after it had been activated. Figure 5b shows an experiment in which, after completing the depletion procedure, the fiber was exposed first to 5 mM Ca^{2+} and after 70 s to 2 μM FCCP. Exposure to Ca^{2+} caused an increase in $[Ca^{2+}]_{myo}$, which reached 300 nM in about 170 s. Exposure to FCCP not only blocked, with a 100 s delay, the increase in $[Ca^{2+}]_{myo}$, but also caused a

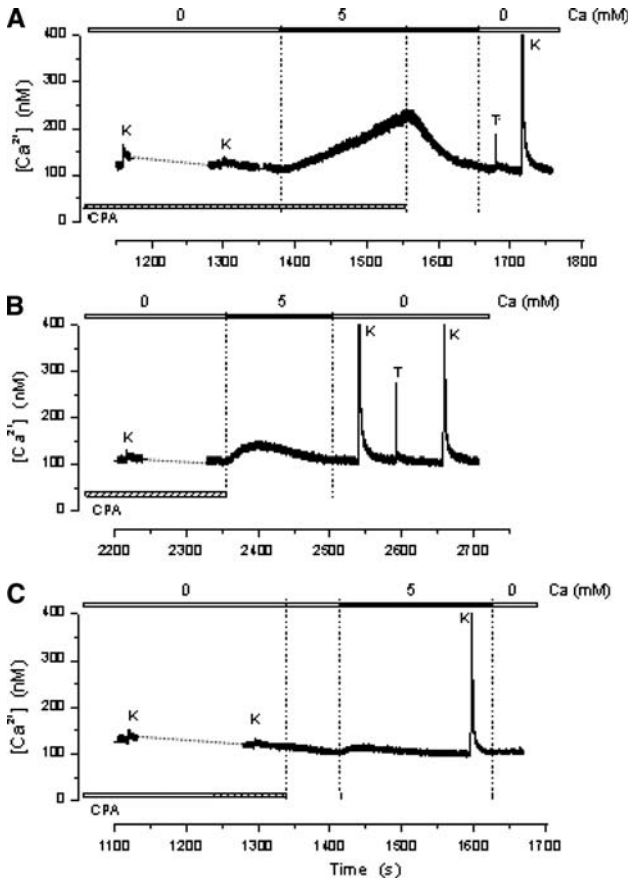

Fig. 3 Reversibility of the CPA effect on the SR Ca^{2+} pump. The three runs in the figure, carried out with different fibers, show that following the depletion procedure, washing out CPA at different times: **a** after, **b** simultaneously or **c** before activating SOCE with 5 mM Ca^{2+}, rapidly reverses or reduces the $[Ca^{2+}]_{myo}$. The results demonstrate that the unpoisoned SR Ca^{2+} pump effectively competes with SOCE

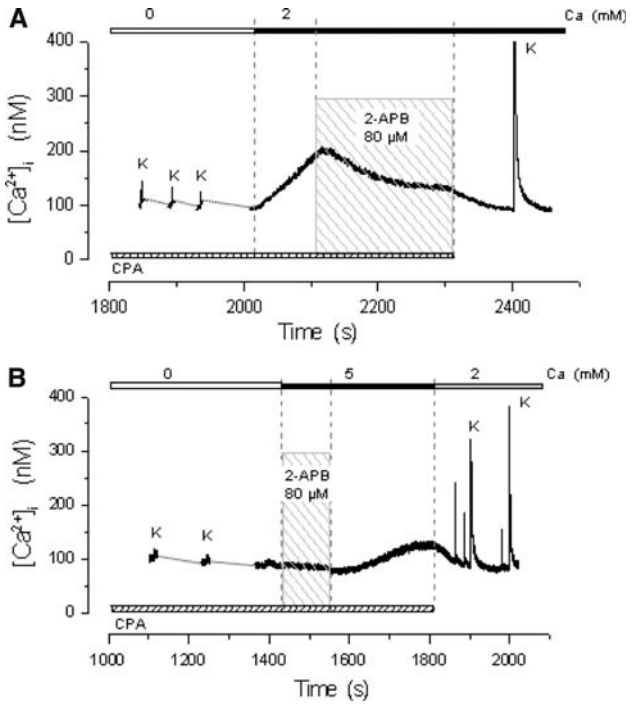

Fig. 4 SOCE blocking by 2-APB. **a** Reversion of the $[Ca^{2+}]_{myo}$ increase by exposure to 80 µM 2-APB. **b** Inhibition of the $[Ca^{2+}]_{myo}$ increase by simultaneous exposure of the fiber to 5 mM Ca^{2+} and 2-APB. A small delayed increase could be observed after washing out the drug

small decrease in its value. The $[Ca^{2+}]_{myo}$ decay was accelerated by washing out CPA, without, however, reaching baseline levels, as has previously been described in the experiments carried out in the absence of FCCP (Fig. 3). Similar results were obtained in three other fibers. The results show that FCCP is still capable of affecting SOCE, even after its activation. Interestingly, it also suggests that FCCP treatment may affect the fiber Ca^{2+} clearance capacity after CPA is removed.

Mitochondrial Ca^{2+} following depletion of Ca^{2+} stores

An important observation resulting from the experiment in Fig. 5a is that after depletion of the SR Ca^{2+} stores, exposure of the fibers to FCCP causes a much smaller increase in the basal $[Ca^{2+}]_{myo}$ than that recently described in rested, non-depleted fibers [23]. The experiment of Fig. 6a shows the effect of FCCP on the basal $[Ca^{2+}]_{myo}$ in a fiber not subjected to the depletion procedure. The experiment shows that myoplasmic Ca^{2+} starts to increase 45 s after exposure to 2 µM FCCP and reaches a level of 234 nM from the 108 nM initial value, whereas, in non-depleted fibers, the mean increase in $[Ca^{2+}]_{myo}$ was 233 ± 14.9 nM, $n = 10$. Figure 6b compares the reduction of Ca^{2+} responses to high K^+, 4-CmC and FCCP observed before and after store depletion. A comparison of the FCCP effect is made between the mean values from two sets of experiments: the value before depletion, taken from a previous work [23], and the value after depletion, taken from this work. In the case of the high K^+ and 4-CmC responses, the values obtained under normal conditions represent a low estimate since in many cases the response peak exceeded the saturation level of our acquisition system. Figure 6b shows that after depletion, the responses to high K^+, 4-CmC and FCCP were reduced by 98.6, 99.4 and 93.5%, respectively. It should be noted that the absolute value of the residual response is rather similar in the three cases: 26.2, 13.1 and 15.2 nM, respectively. This could indicate that following the SR Ca^{2+} depletion procedure, the content of the mitochondria is also reduced. This possibility was explored by measuring the fluorescence of the Ca^{2+}-sensitive dyes CaOr-5N and Rhod-2, before, during and after the depletion procedure. Control experiments (not shown) confirmed that these dyes are highly co-localized with MitoTracker Green, which selectively stains mitochondria and therefore selectively labels mitochondrial Ca^{2+} [20].

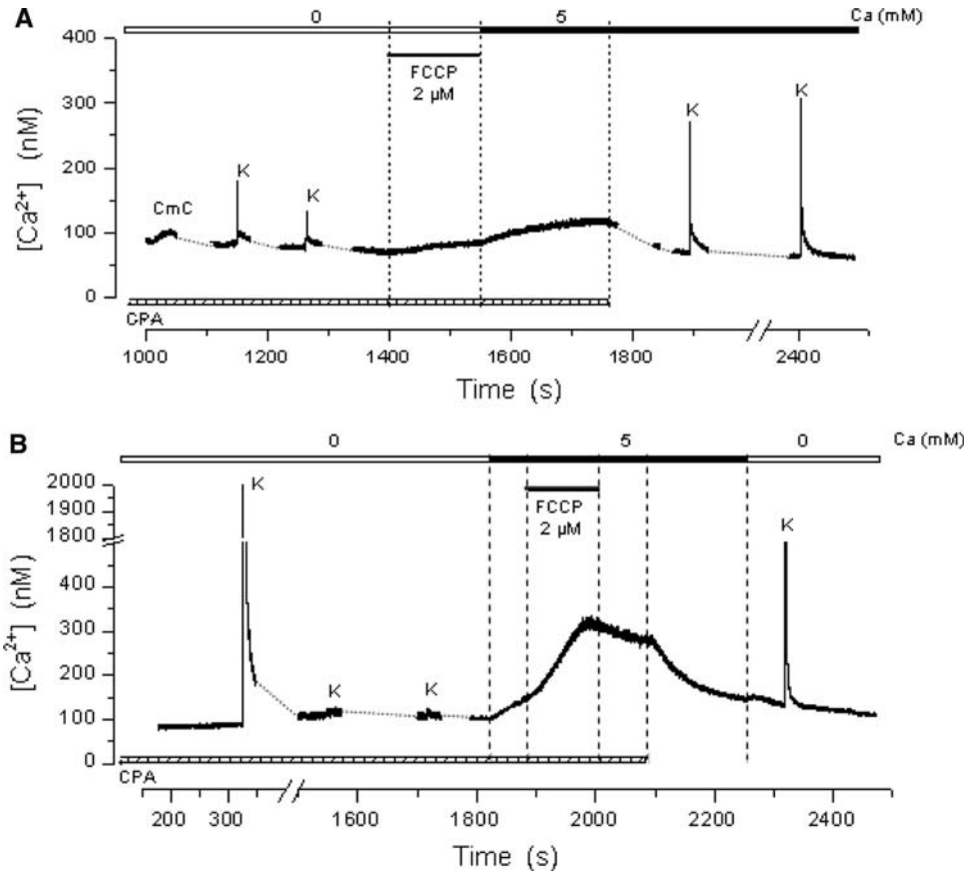

Fig. 5 Inhibition of SOCE by mitochondrial uncoupling. **a** Treatment with FCCP 2 μM effectively reduces SOCE activation. FCCP by itself causes a small increase in the $[Ca^{2+}]_{myo}$. **b** FCCP affects SOCE even after its activation. The experiment shows that the increase in $[Ca^{2+}]_{myo}$ is halted and even reversed by FCCP applied after SOCE activation

The image in Fig. 7a, obtained with a Nikon C1 Confocal Laser Scanning Microscope, shows that most of the Rhod-2 fluorescence originated at the mitochondria level; it is also present in the myoplasm, albeit in a diffuse way. The image in Fig. 7b represents the mask created by the ImageJ 1.41 g Particle Analysis program and shows the mitochondria selected for analysis. Images from the same fiber were acquired at different times during the depletion procedure. The graph in Fig. 7c shows the change of mitochondrial fluorescence value occurring during the depletion procedure. The experimental points in the graph represent the mean (±SEM) value of mitochondria fluorescence, expressed in arbitrary units. The results indicate an increase in mitochondrial Ca^{2+} during the early stages of Ca^{2+} store depletion that later diminishes; equal results were obtained in two additional experiments carried out with CaOr-5N.

A role for the reverse Na^+/Ca^{2+} exchanger during SOCE activation

In view of recent results obtained with human platelets [14], we thought it of interest to explore whether the Na^+/Ca^{2+} exchanger, operating in its reverse mode (Na^+ out/Ca^{2+} in) could have a role in the $[Ca^{2+}]_{myo}$ increase due to SOCE activation in mammalian muscle. Figure 8a shows an experiment in which, following the depletion procedure, SOCE was activated by exposure to 2.5 mM Ca^{2+}, reaching a $[Ca^{2+}]_{myo}$ 250 nM in about 175 s. This increase was interrupted by exposure to 20 μM KB-R7943, a potent but not very specific inhibitor of the reversal mode of Na^+/Ca^{2+} exchanger, causing a partial reverse of the $[Ca^{2+}]_{myo}$ increase. The removal of the inhibitor caused resumption of the $[Ca^{2+}]_{myo}$ increase, reaching a value of approximately 370 nM, at which time the fiber was exposed to a solution in which Na^+ was substituted by Li^+, causing a rapid decrease in the myoplasmic Ca^{2+} concentration. The effect was repeated by again exposing the fiber to a Na^+–$0Na^+$ cycle. It is interesting to note that, when both external Na^+ and Ca^{2+} were washed out, the decay to the initial baseline was not complete and only occurred when the SR Ca^{2+} pump inhibitor CPA was also removed. This protocol was repeated with two other fibers. The effect of Na^+ withdrawal (substituted by Li^+ or $Tris^+$) on the $[Ca^{2+}]_{myo}$ levels was consistently observed in several fibers as shown in Table 2. This result indicates that the myoplasmic Ca^{2+} increase, associated with SOCE activation, depends at least in part on the presence of external Na^+. The possibility that muscle fibers could be loaded with Na^+ during SOCE

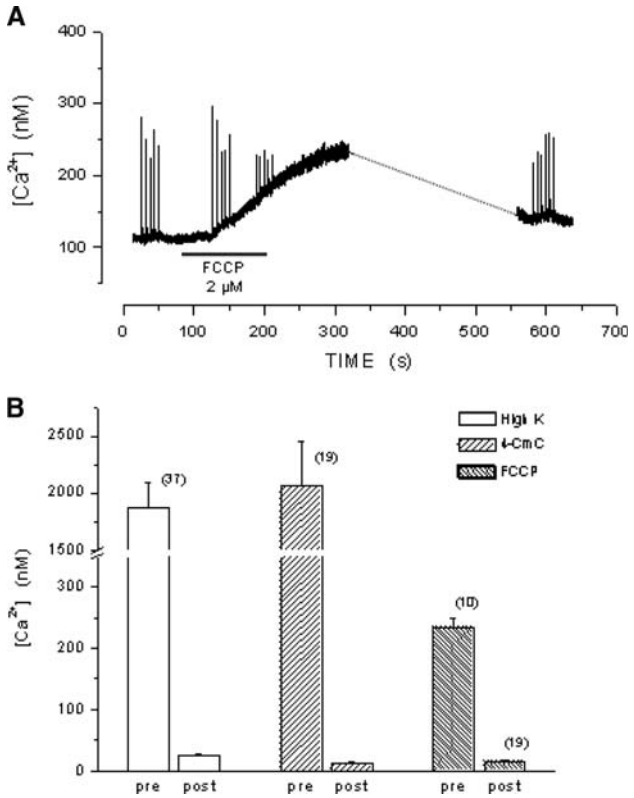

Fig. 6 **a** Effect of FCCP 2 µM on the basal $[Ca^{2+}]_{myo}$ in a non-depleted fiber. **b** Reduction of the $[Ca^{2+}]_{myo}$ increases in response to high K^+, 4-CmC and FCCP after store depletion (column labeled post)

activation was tested. The compound SBFI was used to report intracellular Na^+ increase in one fiber subjected to the same protocol of the experiment in Fig. 8a. In the run shown in Fig. 8b, the changes in myoplasmic Na^+ levels are reported in terms of the 340/380 fluorescence ratio for this dye. It can be observed that following the depletion procedure, when the fiber is exposed to external Ca^{2+}, the internal Na^+ level increases. Exposure of the fiber to the KB-R7943 inhibitor discontinues this increase and perhaps begins its reversal, while external Na^+ withdrawal completely reverses it. Re-adding Na^+ in the external medium causes a new increase in myoplasmic Na^+.

Discussion

SOCE in skeletal muscle fibers

In non-excitable cells, SOCE constitutes a major pathway for Ca^{2+} entry that by interaction with different intracellular Ca^{2+} stores, such as the endoplasmic reticulum and mitochondria, may modulate Ca^{2+} signals [6, 24–27]. SOCE has also been demonstrated in adult skeletal muscle cells [7, 8, 10–12]. In muscle fibers Ca^{2+} transients elicited by electrical stimulation are the most stereotyped signals; the sarcoplasmic reticulum has a protagonist role in the release of the Ca^{2+} necessary for contractile activation and in its sequestration during relaxation. In this scenario, the role of SOCE has yet to be well established. It has recently been proposed that this mechanism could in principle provide a source of Ca^{2+} to replenish intracellular Ca^{2+} stores and avoid their depletion during repetitive activity [11].

In this work SOCE was studied by following the changes in myoplasmic Ca^{2+} concentration by measuring fura-2 fluorescence in mouse muscle fibers whose SR Ca^{2+} stores had been severely depleted and its replenishment blocked by the use of CPA, a potent and reversible inhibitor of the SR Ca^{2+} ATPase. Under these conditions, the maximum rate of

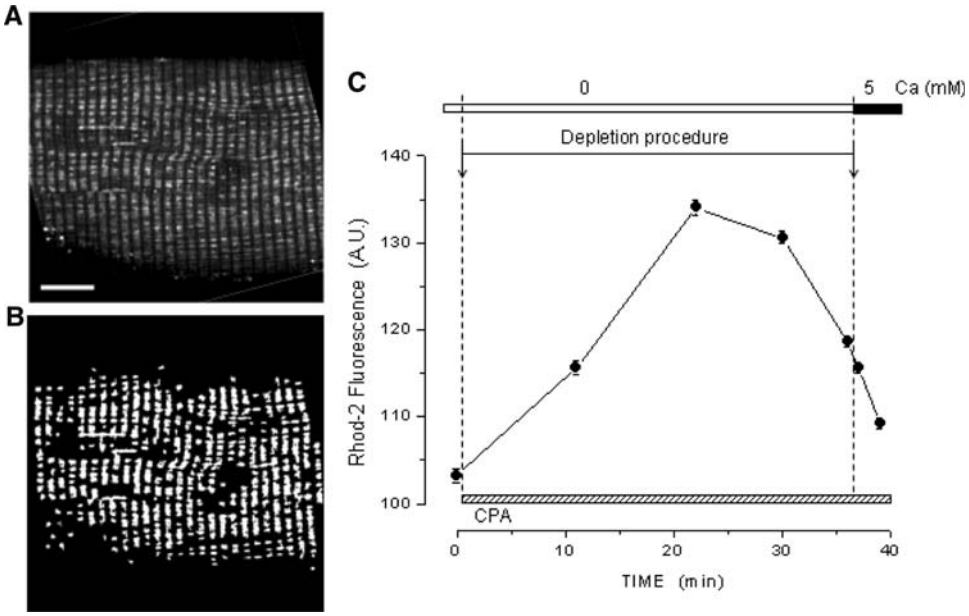

Fig. 7 Variations in $[Ca^{2+}]_{mit}$ during SR Ca^{2+} depletion. **a** A confocal image of a fiber loaded with Rhod-2; **b** A "mask" of the image in **a**, obtained using the Particle Analysis module of the ImageJ program, as explained in the Methods section. **c** The time course of the mean Rhod-2 fluorescence variation of the mitochondria during the depletion procedure. The points represent the mitochondrial fluorescence expressed as arbitrary units (mean ± SEM, $n = 354$). Calibration bar 10 µm

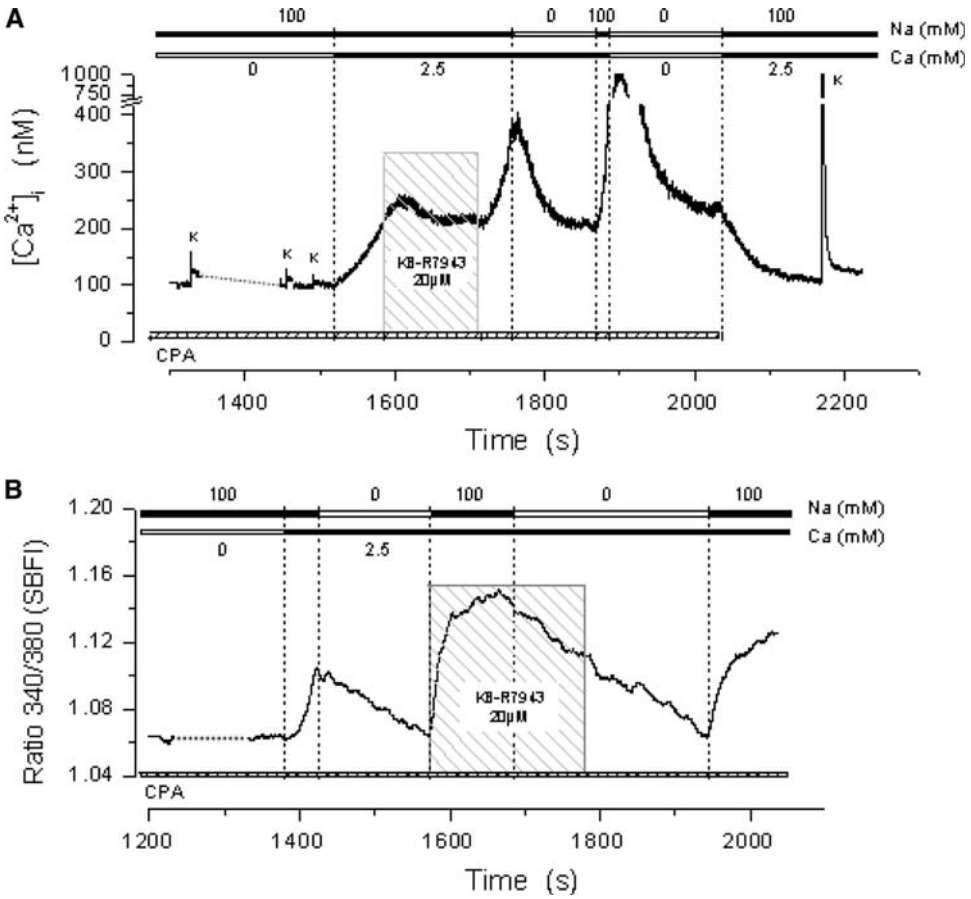

Fig. 8 SOCE dependence on extracellular Na^+. **a** The activation-inhibition cycle on Ca^{2+} entry by SOCE when external Na^+ is substituted by Tris or exposed to the Na^+/Ca^{2+} exchange inhibitor KB-R7943. **b** Changes in cytoplasmic Na^+ in a similar experiment carried out in a different fiber loaded with Na^+ indicator SBFI. The figure demonstrates that following depletion, SOCE activation causes simultaneous increases in cytoplasmic Ca^{2+} and Na^+

Table 2 External sodium effect on SOCE

	$\Delta[Ca^{2+}]$ (nM)	$\Delta[Ca^{2+}]/[Ca^{2+}]_{max}$	*N*
0Na (Li)	−33.8 ± 21.4	0.5 ± 0.10	5
0Na (Tris)	−76.6 ± 6.4	0.6 ± 0.04	16
25Na (Tris)	−62.3 ± 14.2	0.6 ± 0.07	4
50Na (Tris)	−45.0 ± 11.4	0.4 ± 0.06	5

Mean ± SEM, $[Ca^{2+}]_{max}$ value before the withdrawal of external Na^+

$[Ca^{2+}]_{myo}$ increase was 12 nM s^{-1} when extracellular Ca^{2+} was 5 mM. This value is much smaller than that of the directly measured Ca^{2+} flux into the fiber, 16 μM s^{-1}, which was recently determined [11]. Apart from the different techniques and preparations, an additional interesting possibility for this difference could be the presence of undetermined Ca^{2+} sinks in intact fibers affecting our measurements.

Effect of FCCP

An important result of this work is the demonstration that, in adult mouse skeletal muscle fibers, the mitochondrial uncoupler FCCP diminishes SOCE significantly.

The importance of mitochondria in the regulation of SOCE has been demonstrated by the work of various authors [6, 24–27]. In these preparations, mitochondrial poisoning causes inactivation or reduction of Icrac [6, 26, 28]. The work of Parekh and colleagues has shown that Ca^{2+} uptake by fully energized mitochondria is required for Icrac activation by InsP3, under physiological conditions. Mitochondrial poisoning has two simultaneous effects mediated by the Ca^{2+} buffering action: (1) removal of mitochondrial competition with SERCA pumps that facilitates store replenishment, stopping SOCE [29]; (2) reduction of Ca^{2+} uptake by mitochondria increases cytoplasmic Ca^{2+}, thus favoring Ca^{2+}-dependent inactivation of the SOC channels [24]. In our work, the effect of mitochondrial poisoning by FCCP cannot be explained in a similar way because of the widely different experimental conditions. Under these conditions, mitochondrial poisoning may have caused the loss of some signal necessary for SOCE activation or maintenance, in agreement with the proposal [26] that mitochondria may also contribute to SOCE activation by a Ca^{2+} buffering independent mechanism, involving some hitherto unidentified factor produced by functional mitochondria.

The complex mechanisms involved in SOCE activation render it difficult to speculate on the mode of action of unidentified compounds that might interfere with it. However, it has been recently shown that in mice skeletal

muscle, a STIM1-specific antibody highly co-localizes with a RyR1 antibody, indicating the presence of STIM1 molecules in the junctional region of the SR where also mitochondria are closely localized [30]. This proximity should favor an active interaction between mitochondria and the STIM1 and ORAI components of the Icrac.

We also report that in some fibers the responses to high K^+ or to 4-CmC at the end of the experiment were larger than those obtained at its beginning, indicating that in resting state, the SR is not completely filled, in agreement with a previous report showing that the SR of fast twitch muscle is only 1/3 full [31]. This observation, however, is apparently not related to the fact that, under our experimental conditions, there were two modalities of SOCE activation.

Mitochondrial Ca^{2+} during the depletion protocol

Another observation pertains to the increase in myoplasmic Ca^{2+} observed in response to exposure of depleted fibers to FCCP. This increase is smaller than that previously reported [23] for the case of non-depleted fibers, and its magnitude is similar to that of the Ca^{2+} responses to high K^+ or 4-CmC obtained in depleted fibers (see Fig. 6). This could mean either that the $[Ca^{2+}]_{myo}$ increase caused by FCCP originates from the SR and not from the mitochondria, or that the mitochondria content also diminishes following the depletion procedure. Although, the first possibility cannot be totally ruled out, we have presented evidence in favor of the second possibility.

In fact, the confocal experiments suggest that during the first phase of store depletion, the Ca^{2+} content of the mitochondria measured with CaOr-5N or with Rhod-2 increases, but in the final phases of depletion the mitochondrial Ca^{2+} concentration diminishes. A possible explanation for the biphasic change in the Ca^{2+} content of the mitochondrial compartment during acute SR Ca^{2+} depletion is that during the first phase (increased Ca^{2+} content), Ca^{2+} released from the SR by high K^+ or 4-CmC is partially taken into the mitochondria through the mitochondrial calcium uniporter (MCU). The decreased mitochondrial content that occurs when the SR is partially depleted could indicate that it may be determined by the SR Ca^{2+} content, as previously suggested from results obtained under different experimental conditions [32, 33]. In striated muscle, a coupling between SR and mitochondria would be facilitated by the physical proximity of the two structures. Recently, small bridges or *tethers* have been

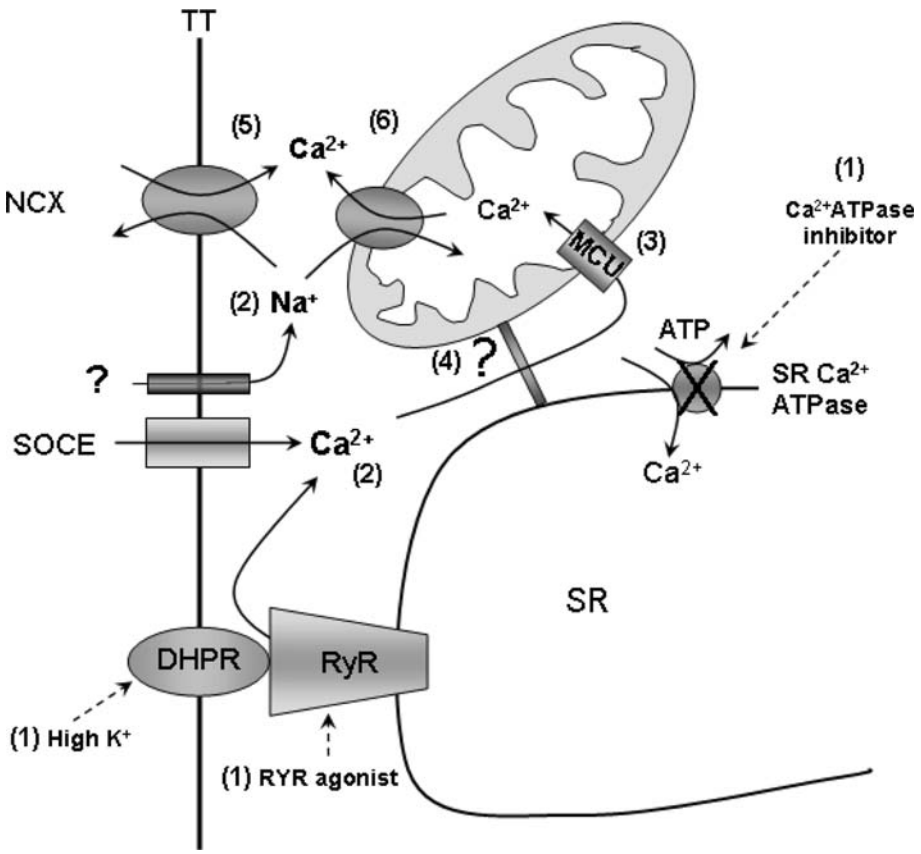

Fig. 9 Schematic diagram of the interrelationships among acute Ca^{2+} depletion of the SR, opening of the SOCE, Ca^{2+} uptake and release from the mitochondrial compartment and Ca^{2+} entry through the reverse plasma membrane Na^+/Ca^{2+} exchange. *1* SR Ca^{2+} depletion procedure. *2* Ca^{2+} entry through SOC and Na^+ entry by an unidentified pathway. *3* Ca^{2+} uptake into the mitochondria through its uniporter following the electrochemical gradient. *4* An unknown step linking mitochondria, SOCE and SR-Ca^{2+} content. *5* Ca^{2+} entry through the electrogenic plasma membrane Na^+/Ca^{2+} exchange and *6* Ca^{2+} release from the mitochondria through its electroneutral Na^+/Ca^{2+} exchange as a consequence of the rise in $[Na^+]_i$ (see text for explanation)

described in skeletal muscle, providing a rather strong link between the outer mitochondrial membrane and SR [34], possibly acting not only as anchors but also as sensors.

A possible role of the Na^+/Ca^{2+} exchange

Finally, we also show that the increase in myoplasmic Ca^{2+} observed after SOCE activation can be partially reversed by external Na^+ withdrawal. This effect could be explained assuming that in muscle fibers, Ca^{2+} entry following SOCE activation is accompanied by an entry of Na^+. In human platelets, it has been shown that Na^+ may enter the cell through the SOCE pathway [14]. However, in rat peritoneal mast cells [5] and in Jurkat T lymphocytes [35], Icrac has been shown to be impermeant to Na^+ when external Ca^{2+} is present. Therefore, we may tentatively assume that Na^+ enters muscle fibers through an unidentified pathway.

The increase in intracellular Na^+, which in principle could reach very high levels in microdomains near the membrane, possibly increases Ca^{2+} entry by activation of the Na^+/Ca^{2+} exchanger in its reverse mode. This could explain why Na^+ withdrawal causes a decrease in the Ca^{2+} levels attained during SOCE. Preliminary experiments carried out with the Na^+/Ca^{2+} exchanger inhibitor KB-R7943 and with the Na^+-sensitive fluorescent dye SBFI appear to support this possibility. An increase in intracellular Na^+ could also facilitate Ca^{2+} efflux from the mitochondria through the activation of the mitochondrial Na^+/Ca^{2+} exchanger, as suggested above.

Apart from the FCCP effect on SOCE, for which we do not have a plausible explanation, the other major finding obtained in this work is summarized in the diagram in Fig. 9. Depletion of SR Ca^{2+} content by inhibitors of the SR Ca^{2+}-ATPase, agonists of RYR and/or repetitive plasma membrane depolarization with high external potassium solutions (1) induces the opening of SOCE (2), thus allowing Ca^{2+} entry into the myoplasm, which in part is taken up by the mitochondrial compartment via the mitochondrial calcium uniporter, MCU (3), as clearly shown in our confocal results. Although the link between the state of the mitochondrial compartment, SOCE, SR Ca^{2+} content and release is unknown (4), our data clearly show an interrelationship among them. The increase of $[Na^+]$ in the myoplasm and the sodium dependency of the intracellular Ca^{2+} signal indicates that activation of the plasma membrane electrogenic Na^+/Ca^{2+} exchange could contribute to the overall Ca^{2+} increase in the myoplasm when SOCE is activated [5]. Finally, Ca^{2+} release from the mitochondria through its electro neutral Na^+/Ca^{2+} exchange might also contribute to the overall Ca^{2+} signal. Further work is in progress in our laboratory to characterize the relationship between these different mechanisms.

Acknowledgments We acknowledge the kind gift of CaOr-5 N by Dr. Ariel Escobar. This work was supported by FONACIT grant G-2001000637.

References

1. Putney JW Jr (1986) A model for receptor-regulated calcium entry. Cell Calcium 7:1–12. doi:10.1016/0143-4160(86)90026-6
2. Hoth M, Penner R (1992) Depletion of intracellular calcium stores activates a calcium current in mast cells. Nature 355:353–356. doi:10.1038/355353a0
3. Parekh AB, Penner R (1995) Activation of store-operated calcium influx at resting InsP3 levels by sensitization of the InsP3 receptor in rat basophilic leukaemia cells. J Physiol 489(Pt 2):377–382
4. Fierro L, Parekh AB (2000) Substantial depletion of the intracellular Ca^{2+} stores is required for macroscopic activation of the Ca^{2+} release-activated Ca^{2+} current in rat basophilic leukaemia cells. J Physiol 522:247–257. doi:10.1111/j.1469-7793.2000.t01-1-00247.x
5. Hoth M, Penner R (1993) Calcium release-activated calcium current in rat mast cells. J Physiol 465:359–386
6. Gilabert JA, Parekh AB (2000) Respiring mitochondria determine the pattern of activation and inactivation of the store-operated Ca^{2+} current Icrac. EMBO J 19:6401–6407. doi:10.1093/emboj/19.23.6401
7. Kurebayashi N, Ogawa Y (2001) Depletion of Ca^{2+} in the sarcoplasmic reticulum stimulates Ca^{2+} entry into mouse skeletal muscle fibres. J Physiol 533:185–199. doi:10.1111/j.1469-7793.2001.0185b.x
8. Gonzalez Narvaez AA, Castillo A (2007) Ca^{2+} store determines gating of store operated calcium entry in mammalian skeletal muscle. J Muscle Res Cell Motil 28:105–113. doi:10.1007/s10974-007-9105-x
9. Ma J, Pan Z (2003) Retrograde activation of store-operated calcium channel. Cell Calcium. 33:375–384. doi:10.1016/S0143-4160(03)00050-2
10. Ducret T, Vandebrouck C, Cao ML, Lebacq J, Gailly P (2006) Functional role of store-operated and stretch-activated channels in murine adult skeletal muscle fibres. J Physiol 575:913–924. doi:10.1113/jphysiol.2006.115154
11. Launikonis BS, Rios E (2007) Store-operated Ca^{2+} entry during intracellular Ca^{2+} release in mammalian skeletal muscle. J Physiol 583:81–97. doi:10.1113/jphysiol.2007.135046
12. Ma J, Pan Z (2003) Junctional membrane structure and store operated calcium entry in muscle cells. Front Biosci 8:d242–d255. doi:10.2741/977
13. Allard B, Couchoux H, Pouvreau S, Jacquemond V (2006) Sarcoplasmic reticulum Ca^{2+} release and depletion fail to affect sarcolemmal ion channel activity in mouse skeletal muscle. J Physiol 575:68–81. doi:10.1113/jphysiol.2006.112367
14. Harper AG, Sage SO (2007) A key role for reverse Na^+/Ca^{2+} exchange influenced by the actin cytoskeleton in store-operated Ca^{2+} entry in human platelets: evidence against the de novo conformational coupling hypothesis. Cell Calcium 42:606–617. doi:10.1016/j.ceca.2007.02.004
15. Carroll SL, Klein M, Schneider MF (1995) Calcium transients in intact rat skeletal muscle fibers in agarose gel. Am J Physiol 269:C28–C34
16. Capote J, Bolaños P, Schuhmeier RP, Melzer W, Caputo C (2005) Calcium transients in developing mouse skeletal muscle fibres. J Physiol 564:451–464. doi:10.1113/jphysiol.2004.081034
17. Grynkiewicz G, Poenie M, Tsien RY (1985) A new generation of Ca^{2+} indicators with greatly improved fluorescence properties. J Biol Chem 260:3440–3450

18. Klein MG, Simon BJ, Szucs G, Schneider MF (1988) Simultaneous recording of calcium transients in skeletal muscle using high- and low-affinity calcium indicators. Biophys J 53:971–988. doi:10.1016/S0006-3495(88)83178-3
19. Yeung EW, Ballard HJ, Bourreau JP, Allen DG (2003) Intracellular sodium in mammalian muscle fibers after eccentric contractions. J Appl Physiol 94:2475–2482
20. Bolaños P, Guillen A, Rojas H, Boncompagni S, Caputo C (2008) The use of Calcium Orange-5N as a specific marker of mitochondrial Ca^{2+} in mouse skeletal muscle fibers. Pflugers Arch 455:721–731. doi:10.1007/s00424-007-0312-5
21. Zhao M, Hollingworth S, Baylor SM (1996) Properties of tri- and tetracarboxylate Ca^{2+} indicators in frog skeletal muscle fibers. Biophys J 70:896–916. doi:10.1016/S0006-3495(96)79633-9
22. Fasolato C, Hoth M, Penner R (1993) Multiple mechanisms of manganese-induced quenching of fura-2 fluorescence in rat mast cells. Pflugers Arch 423:225–231. doi:10.1007/BF00374399
23. Caputo C, Bolaños P (2008) Effect of mitochondria poisoning by FCCP on Ca^{2+} signaling in mouse skeletal muscle fibers. Pflugers Arch 455:733–743. doi:10.1007/s00424-007-0317-0
24. Hoth M, Button DC, Lewis RS (2000) Mitochondrial control of calcium-channel gating: a mechanism for sustained signaling and transcriptional activation in T lymphocytes. Proc Natl Acad Sci USA 97:10607–10612. doi:10.1073/pnas.180143997
25. Gilabert JA, Bakowski D, Parekh AB (2001) Energized mitochondria increase the dynamic range over which inositol 1, 4, 5-trisphosphate activates store-operated calcium influx. EMBO J 10:2672–2679. doi:10.1093/emboj/20.11.2672
26. Glitsch MD, Bakowski D, Parekh AB (2002) Store-operated Ca^{2+} entry depends on mitochondrial Ca^{2+} uptake. EMBO J 21:6744–6754. doi:10.1093/emboj/cdf675
27. Parekh AB (2003) Mitochondrial regulation of intracellular Ca^{2+} signaling: more than just simple Ca^{2+} buffers. News Physiol Sci 18:252–256
28. Hoth M, Fanger CM, Lewis RS (1997) Mitochondrial regulation of store-operated calcium signaling in T lymphocytes. J Cell Biol 137:633–648. doi:10.1083/jcb.137.3.633
29. Parekh AB (2003) Store-operated Ca^{2+} entry: dynamic interplay between endoplasmic reticulum, mitochondria and plasma membrane. J Physiol 547:333–348. doi:10.1113/jphysiol.2002.034140
30. Stiber J, Hawkins A, Zhang ZS, Wang S, Burch J, Graham V, Ward CC, Seth M, Finch E, Malouf N, Williams RS, Eu JP, Rosenberg P (2008) STIM1 signalling controls store-operated calcium entry required for development and contractile function in skeletal muscle. Nat Cell Biol 10:688–697. doi:10.1038/ncb1731
31. Fryer MW, Stephenson DG (1996) Total and sarcoplasmic reticulum calcium contents of skinned fibres from rat skeletal muscle. J Physiol 493(Pt 2):357–370
32. Rudolf R, Mongillo M, Magalhaes PJ, Pozzan T (2004) In vivo monitoring of Ca^{2+} uptake into mitochondria of mouse skeletal muscle during contraction. J Cell Biol 166:527–536. doi:10.1083/jcb.200403102
33. Vandebrouck A, Ducret T, Basset O, Sebille S, Raymond G, Ruegg U, Gailly P, Cognard C, Constantin B (2006) Regulation of store-operated calcium entries and mitochondrial uptake by minidystrophin expression in cultured myotubes. Faseb J 20:136–138
34. Boncompagni S, Rossi AE, Micaroni M, Beznoussenko GV, Polishchuk RS, Dirksen RT, Protasi F (2009) Mitochondria are linked to calcium stores in striated muscle by developmentally regulated tethering structures. Mol Biol Cell 20:1058–1067. doi:10.1091/mbc.E08-07-0783
35. Lepple-Wienhues A, Cahalan MD (1996) Conductance and permeation of monovalent cations through depletion-activated Ca2+ channels (ICRAC) in Jurkat T cells. Biophys J 71:787–794. doi:10.1016/S0006-3495(96)79278-0